Neuron, Vol. 31, 713–726, September 13, 2001, Copyright ©2001 by Cell Press

APP Processing and Synaptic Plasticity in *Presenilin-1* Conditional Knockout Mice

Huakui Yu,[1,8] Carlos A. Saura,[1,8] Se-Young Choi,[3] Linus D. Sun,[4] Xudong Yang,[1] Melissa Handler,[1] Takeshi Kawarabayashi,[5] Linda Younkin,[5] Bogdan Fedeles,[4] Matthew A. Wilson,[4] Steve Younkin,[5] Eric R. Kandel,[6] Alfredo Kirkwood,[3] and Jie Shen[1, 2,7]

[1]Center for Neurologic Diseases
Brigham and Women's Hospital
[2]Program in Neuroscience
Harvard Medical School
Boston, Massachusetts 02115
[3]Mind/Brain Institute
Johns Hopkins University
Baltimore, Maryland 21218
[4]Department of Brain and Cognitive Sciences
Center for Learning and Memory
Massachusetts Institute of Technology
Cambridge, Massachusetts 02138
[5]Mayo Clinic Jacksonville
Jacksonville, Florida 32224
[6]Howard Hughes Medical Institute
Center for Neurobiology and Behavior
Columbia University
New York, New York 10032

Summary

We have developed a *presenilin-1* (*PS1*) conditional knockout mouse (cKO), in which PS1 inactivation is restricted to the postnatal forebrain. The *PS1* cKO mouse is viable and exhibits no gross abnormalities. The carboxy-terminal fragments of the amyloid precursor protein differentially accumulate in the cerebral cortex of cKO mice, while generation of β-amyloid peptides is reduced. Expression of Notch downstream effector genes, *Hes1*, *Hes5*, and *Dll1*, is unaffected in the cKO cortex. Although basal synaptic transmission, long-term potentiation, and long-term depression at hippocampal area CA1 synapses are normal, the *PS1* cKO mice exhibit subtle but significant deficits in long-term spatial memory. These results demonstrate that inactivation of PS1 function in the adult cerebral cortex leads to reduced Aβ generation and subtle cognitive deficits without affecting expression of Notch downstream genes.

Introduction

Mutations in Presenilin-1 (PS1) are the most common cause of early-onset familial Alzheimer's disease (FAD). Accumulation and deposition of β-amyloid (Aβ) peptides in the cerebral cortex is an early and central process in the pathogenesis of AD. The Aβ peptides are generated from the amyloid precursor protein (APP) as a result of sequential proteolytic cleavages by β- and γ-secretases, which are therefore prime targets for therapeutic intervention. β-secretase (BACE) was recently identified as a novel aspartyl protease, while γ-secretase was found to be closely associated with PS1. The generation of Aβ peptides is markedly reduced in cultured *PS1*$^{-/-}$ neurons (De Strooper et al., 1998). Conversely, FAD-linked PS1 mutations invariably lead to increased production of the particularly amyloidogenic species Aβ42 (Duff et al., 1996; Jarrett et al., 1993; Scheuner et al., 1996). It has been postulated that PS1 may itself possess γ-secretase activity (Wolfe et al., 1999), a notion that is supported by the direct binding of PS1 by peptidomimetic γ-secretase inhibitors (Esler et al., 2000; Li et al., 2000). These findings have raised the possibility that PS1 may represent an attractive target for anti-amyloidogenic therapy.

The feasibility of PS1 as a therapeutic target for AD depends critically on the effects of reduced PS1 function in the adult brain. Due to the perinatal lethality of *PS1*$^{-/-}$ mice, however, previous studies on APP processing in the absence of PS1 have relied on cultured neurons derived from the embryonic *PS1*$^{-/-}$ brain. In addition to its role in APP processing, our previous studies of *PS1*$^{-/-}$ mice showed that PS1 exerts pleiotropic effects during brain development, including the regulation of neurogenesis and Notch signaling (Handler et al., 2000; Shen et al., 1997). In the absence of PS1, neural progenitor cells differentiate prematurely into postmitotic neurons, leading to early depletion of the progenitor cells and subsequently a smaller neuronal population (Handler et al., 2000). Furthermore, Notch signaling is reduced in the *PS1*$^{-/-}$ embryonic brain, as indicated by reduced *Hes5* expression and increased *Dll1* expression (Handler et al., 2000). PS1 appears to influence Notch signaling by regulating the generation of the intracellular domain of Notch1 (NICD) (De Strooper et al., 1999; Song et al., 1999), which translocates to the nucleus to stimulate transcription of downstream effector genes. The role of PS1 in the adult brain, however, remains unknown due to the perinatal lethality of the *PS1*$^{-/-}$ mouse. Recently, mutations in the PS1 homologs in *C. elegans*, sel-12 and hop-1, have been found to lead to defects in temperature memory and the neuritic morphology of two cholinergic interneurons, indicating an involvement of PS1 in neuronal function (Wittenburg et al., 2000).

To investigate the effects of PS1 inactivation on APP processing, the Notch signaling pathway, and synaptic and cognitive function in the adult brain, we employed the Cre/loxP recombination system to develop a *PS1* conditional knockout (cKO) mouse. Using this strategy, PS1 expression is progressively eliminated in the cortex of cKO mice beginning in the third postnatal week. In the adult cerebral cortex of cKO mice, levels of Aβ40 and Aβ42 are differentially reduced, while levels of the APP C-terminal fragments (CTFs) are differentially increased. Surprisingly, expression of the Notch downstream effector genes, *Hes1*, *Hes5*, and *Dll1*, is unaffected in the cortex of cKO mice. Basal synaptic transmission and synaptic plasticity in hippocampal area CA1 are normal, but the *PS1* cKO mice exhibit

[7]Correspondence: jshen@rics.bwh.harvard.edu
[8]These authors contributed equally to this work.

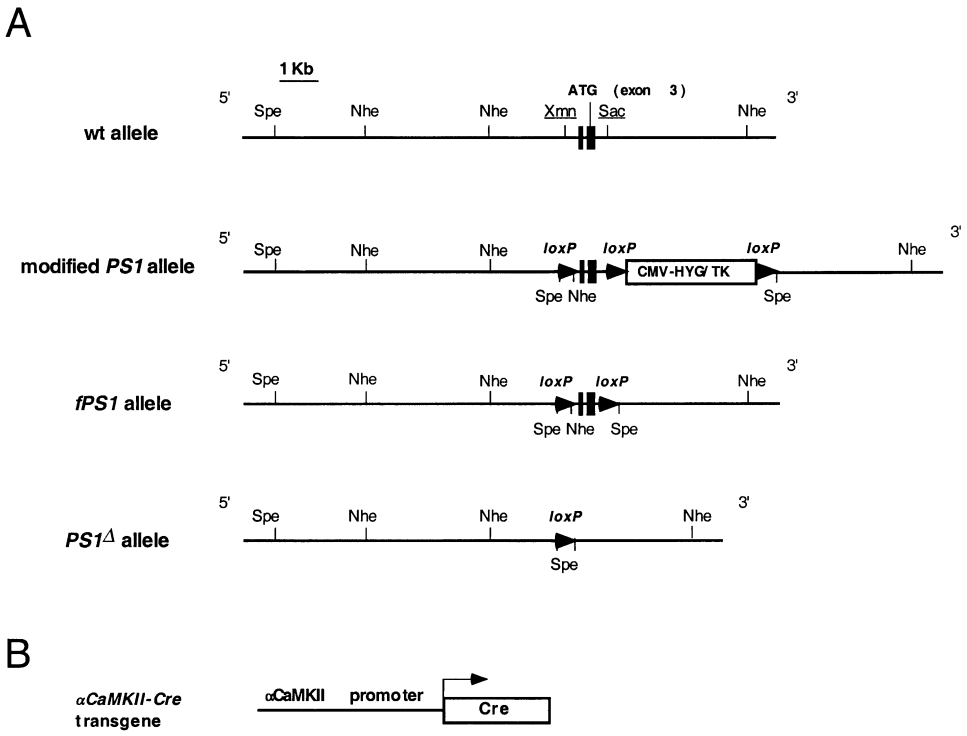

Figure 1. Generation of the Floxed *PS1* and the α*CaMKII-Cre* Transgenic Mice

(A) Schematic representation of the wild-type *PS1* genomic region encompassing exons 2 and 3 and the modified *PS1* alleles. The black boxes represent *PS1* exons 2 and 3, and exon 3 contains the start ATG codon. The modified *PS1* allele contains a loxP site in *PS1* intron 1 and a floxed CMV-HYG/TK selection cassette in intron 3. The floxed selection cassette is removed in the *fPS1* allele, while the entire floxed region including *PS1* exons 2 and 3 is excised in the $PS1^{\Delta}$ allele.

(B) Schematic representation of the α*CaMKII-Cre* transgene (not drawn to scale). The transgene contains a ~8.5 kb segment of the α*CaMKII* promoter, a hybrid 5′ intron, cDNA encoding Cre recombinase, and the SV40 polyadenylation signal.

subtle deficits in spatial reference memory. These results indicate that disruption of PS1 function in the adult brain results in reduced Aβ generation and subtle cognitive impairment.

Results

Generation and Characterization of the *PS1* cKO Mouse

To achieve the selective disruption of PS1 in the cerebral cortex (neocortex and hippocampus) during postnatal life, we employed the recently developed Cre/loxP recombination technology. We first generated a floxed *PS1* mouse, in which *PS1* exons 2 and 3 are flanked by two *loxP* sites (Figure 1A). Using homologous recombination in embryonic stem (ES) cells, we generated a modified *PS1* allele, in which a *loxP* site and a floxed drug selection cassette were introduced into *PS1* introns 1 and 3, respectively (Figure 1A). The floxed *PS1* allele (*fPS1*) and the $PS1^{\Delta}$ allele were then generated by transient transfection of a cDNA encoding Cre recombinase, which mediates site-specific recombination between two *loxP* sites (Yu et al., 2000). ES cells carrying either the *fPS1* or the $PS1^{\Delta}$ allele were injected into mouse blastocysts to generate chimeric mice, which were then used to generate heterozygous and homozygous *fPS1* and $PS1^{\Delta}$ mice. We also generated a *Cre* transgenic mouse (*CaM-Cre*), in which Cre recombinase is expressed selectively in pyramidal neurons of the postnatal forebrain under the control of the α-calcium-calmodulin-dependent kinase II promoter (Figure 1B) (Mayford et al., 1996; Minichiello et al., 1999). The *PS1* conditional knockout (cKO) mouse was then generated by crossing the *fPS1* mouse to the *CaM-Cre* transgenic mouse.

To determine whether the introduction of the *loxP* sites into *PS1* introns affects transcription and/or splicing of *PS1* mRNA, we performed Northern and RT-PCR analyses and found that the level and the size of *PS1* transcripts are unaltered in homozygous *fPS1* mice (Figure 2A and data not shown). The homozygous $PS1^{\Delta}$ mice exhibit phenotypes indistinguishable from those of the $PS1^{-/-}$ mice that we previously reported, confirming that excision of the floxed region results in a *PS1* null allele (Shen et al., 1997). Northern analysis of $PS1^{\Delta}$ mice revealed greatly reduced levels of a smaller *PS1* transcript, indicating that the *PS1* transcript lacking exons 2 and 3 is highly unstable or that important transcriptional regulatory sequences reside within this region (Figure 2A).

Spatial and temporal inactivation of *PS1* expression in cKO mice was examined by Northern, Western, and in situ hybridization analyses. Northern analysis showed a marked reduction in the level of *PS1* mRNA in the cortex (neocortex and hippocampus) of cKO mice at the age of 6 weeks, though residual *PS1* transcripts were

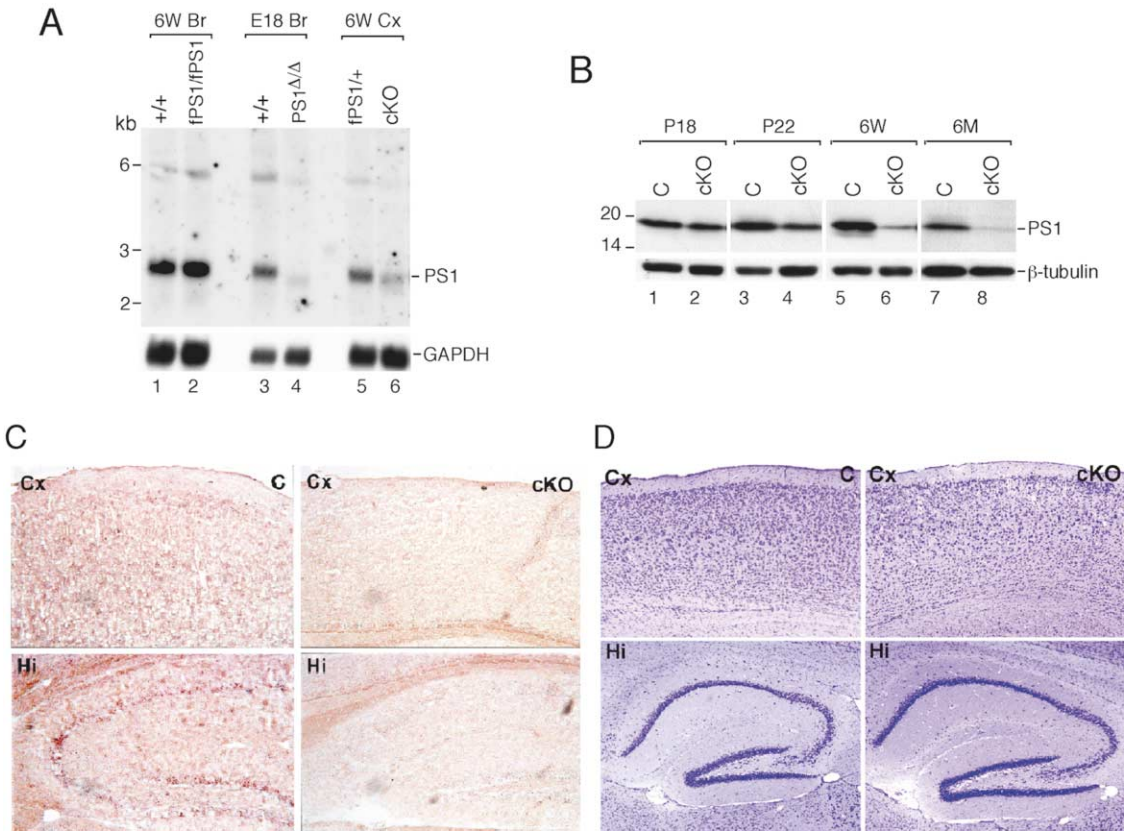

Figure 2. Spatially and Temporally Specific Inactivation of *PS1* in cKO Mice

(A) Northern analysis of *PS1* transcripts in *fPS1/fPS1*, *PS1*$^{\Delta/\Delta}$, and *PS1* cKO mice. Total RNA was prepared from the brains of *fPS1/fPS1* and littermate control (+/+) mice at the age of 6 weeks (lanes 1 and 2), the brains of *PS1*$^{\Delta/\Delta}$ and littermate control (+/+) mice at embryonic day 18 (lanes 3 and 4), and the cortex (neocortex and hippocampus) of cKO (*PS1*$^{\Delta}$*/fPS1;CaM-Cre*) and littermate control (*fPS1/*+) mice at the age of 6 weeks (lanes 5 and 6), and then hybridized with a *PS1* cDNA probe. The same blot was then hybridized with a control probe, *GAPDH*, to normalize the amounts of RNA in each lane.

(B) Progressive elimination of PS1 CTFs in the cKO cortex. Brain homogenate from the cortex of cKO (*PS1*$^{\Delta}$*/fPS1;CaM-Cre*) and littermate control (C) (*fPS1/*+ or *fPS1/fPS1*) mice at the ages of P18, P22, 6 weeks, and 6 months was immunoblotted with antiserum raised against the loop region of PS1 (Thinakaran et al., 1996). The blot was then incubated with β-tubulin antibody to normalize the amounts of protein in each lane.

(C) In situ hybridization analysis of *PS1* expression in the neocortex and hippocampus of *PS1* cKO and control mice. Sagittal brain sections (10 μm) of *PS1* cKO (*PS1*$^{\Delta}$*/fPS1;CaM-Cre*) and littermate control (*PS1*$^{\Delta}$*/fPS1*) mice at the age of 3 months were hybridized with a digoxigenin-labeled probe specific for *PS1* exons 2 and 3. Expression of *PS1* transcripts is largely eliminated in the hippocampus and neocortex of the *PS1* cKO brain.

(D) Normal gross morphology of the hippocampus and neocortex of the cKO mouse. Sagittal brain sections (12 μm) of *PS1* cKO and littermate control mice at the age of 3 months were stained with cresyl violet. The gross morphology of the cKO brain is indistinguishable from that of the control.

still detectable (Figure 2A). Since the majority of endogenous PS1 undergoes endoproteolytic processing into 27 kDa N-terminal and 18 kDa C-terminal fragments (CTF), we examined the level of PS1 CTF by Western analysis. The level of PS1 CTF in the cortex is slightly reduced at postnatal day 18 (P18) and further reduced at P22 (Figure 2B). By the ages of 6 weeks and 6 months, very low levels of PS1 CTF were detected in the cortex of cKO mice, while the level of PS1 CTF was unchanged in the cerebellum and brain stem (Figure 2B and data not shown). These results indicate a selective elimination of PS1 expression in the cortex of *PS1* cKO mice beginning at P18. The residual amount of PS1 observed in the cortex of cKO mice is due to its expression in glial cell types (Lah et al., 1997) and possibly a small population of neurons lacking Cre expression. We further performed in situ hybridization on brain sections of *PS1* cKO and control mice at the age of 3 months using a digoxigenin-labeled probe specific for *PS1* exons 2 and 3. We found that *PS1* is expressed at high levels in the hippocampus and at lower levels in the neocortex of the control brain, while its expression in the cKO brain is eliminated (Figure 2C).

In contrast to *PS1*$^{-/-}$ mice, the *PS1* cKO mouse is viable with no obvious phenotypic abnormalities. Nissl staining of the brain sections of cKO mice at the ages of P18, 20, 22, and 3 months (Figure 2D) also revealed no gross abnormalities. Despite large numbers of reports that have suggested a role for PS1 in apoptosis using various cell culture systems, we failed to detect an increase in apoptosis in the cerebral cortex of cKO mice. Bisbenzimide staining and TUNEL analysis of the

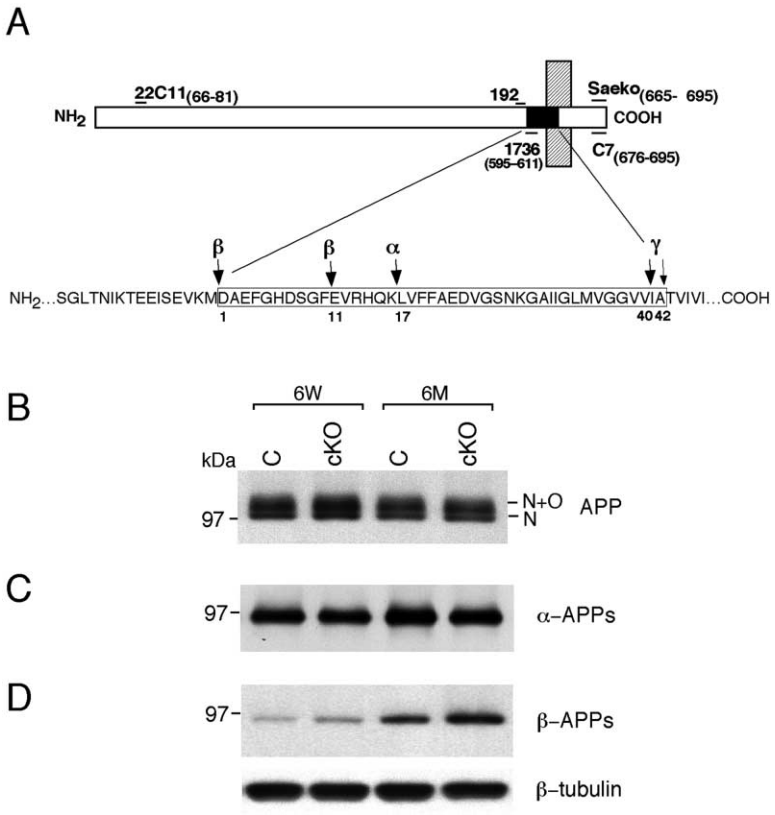

Figure 3. Unchanged Levels of α- and β-APPs in *PS1* cKO Mice

(A) Schematic representation of APP and the amino acid sequence comprising the Aβ region. A single transmembrane domain is indicated by the vertical hatched bar, while the Aβ region is indicated by the filled black box. Antibodies raised against various regions of APP are shown. The α-, β-, and γ-cleavage sites on APP are indicated by vertical arrows.

(B) Western analysis of full-length APP. Levels of full-length APP, which were measured by Western using the "Saeko" antiserum (Kawarabayashi et al., 1996), are similar in the cortex of both *PS1* cKO and control mice at the ages of 6 weeks (6W) and 6 months (6M). "N" and "O" denote glycosylation at the NH_2 and OH groups of Asn and Ser/Thr residues, respectively.

(C) IP-Western analysis of α-APPs. α-APPs was detected by IP with antiserum 1736 followed by Western using antibody 22C11. Levels of α-APPs are similar in the cortex of cKO and control mice at the ages of 6 weeks and 6 months.

(D) Western analysis of β-APPs. β-APPs was detected by antibody 192, which is specific for the C terminus of β-APPs. Levels of β-APPs are similar in the cortex of *PS1* cKO and control mice at the ages of 6 weeks and 6 months. The level of β-APPs is upregulated in the cortex of both *PS1* cKO and control mice from the age of 6 weeks to the age of 6 months. The same immunoblot was incubated with β-tubulin antibody to confirm similar amounts of total protein loaded in each lane. I^{125}-labeled antibodies were also used in Western analysis to measure levels of β-APPs more quantitatively, and no significant differences between the cKO and control cortex were found.

cortex of control and cKO mice at the ages of P18, P20, P22, and 3 months showed no significant difference in the low number of apoptotic cells detected for each genotype (data not shown).

Altered APP Processing and Reduced Aβ Generation

To investigate the role of PS1 in APP processing in the adult cerebral cortex, we used a panel of well-characterized antibodies against APP to examine levels of the APP ectodomains (α-APPs and β-APPs) and membrane bound CTFs (α-CTF and β-CTF) generated by α- and β-secretase cleavage (Figure 3A). β-secretase (BACE1) has been shown to cleave APP at the +1 (Asp) and +11 (Glu) sites of Aβ (Figure 3A) (Cai et al., 2001; Luo et al., 2001). Western analysis showed that the level of the full-length APP is unchanged in the adult cortex lacking PS1 (Figure 3B). Immunoprecipitation (IP) with an antiserum specific for the α-APPs, followed by Western blotting using the antibody 22C11, showed similar levels of the α-APPs in the cortex of cKO and littermate control mice (Figure 3C). Western analysis of β-APPs using an antiserum specific for β-APPs also showed similar levels of the β-APPs in the cKO cortex compared to the control (Figure 3D). These results indicate that PS1 is not involved in the regulation of α- and β-secretase cleavage of APP.

We then performed Western analysis using an antiserum ("Saeko") raised against the C-terminal region of APP to measure the level of the APP CTFs in the cortex, and found that the CTFs accumulate in the cortex of cKO mice in an age-dependent manner (Figure 4A). At P18, the level of the CTFs is slightly higher in the cKO cortex relative to the littermate control. At P22, levels of the CTFs are further increased, consistent with the reduction in the level of PS1 (Figure 2B). At the ages of 6 weeks and 6 months, there is a striking progressive accumulation of the CTFs in the cKO cortex (Figure 4A). Five distinct CTF species were detected in the cortex of cKO and littermate control mice (Figure 4A, lanes 1–8), as previously reported (Buxbaum et al., 1998), while only three APP CTF species were detected in CHO cells transfected with the human wild-type *APP* cDNA (Figure 4A, lane 11). The additional APP CTF species in the brain are phosphorylated forms of the α- and β-CTFs, as they disappear following phosphatase treatment (Figure 4A, lanes 9 and 10). The three CTF species in CHO cells and mouse cortex following phosphatase treatment represent the α-CTF (C83), which is cleaved at +17 (Leu) of Aβ, and the β-CTFs (C99 and C89), which are cleaved at +1 (Asp) and +11 (Glu) of Aβ, respectively (Figure 3A) (Cai et al., 2001; Luo et al., 2001; Simons et al., 1996).

To quantify the increase of the APP CTFs, we performed Western analysis using serial dilutions of cKO brain lysate at the age of 6 months (Figure 4B). We estimate that the levels of C83 and C89 are increased approximately 30-fold, relative to the control, while the increase in the level of C99 is approximately 3-fold. Since

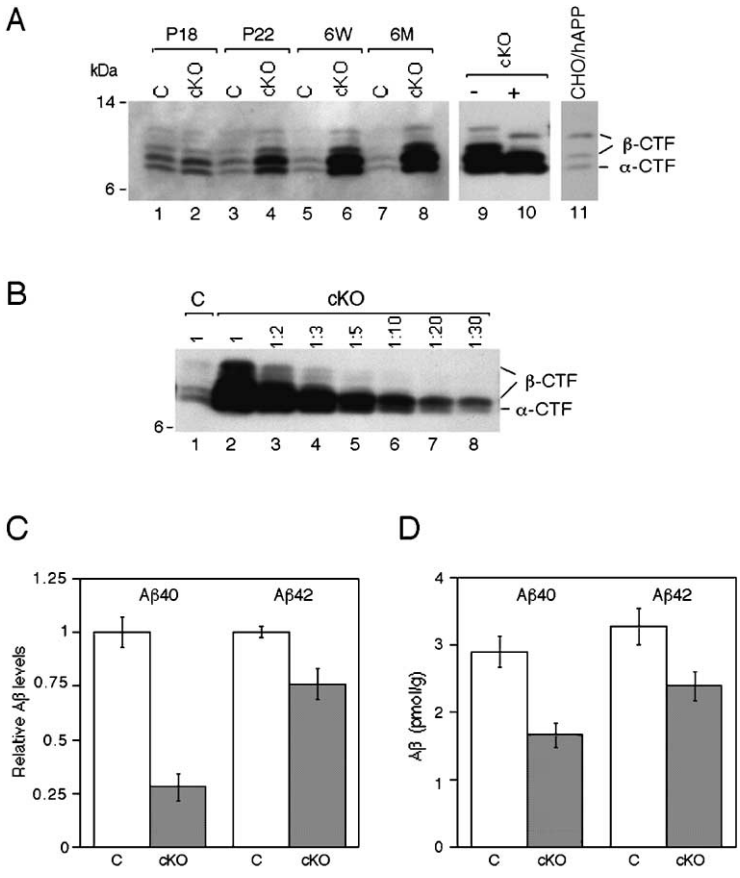

Figure 4. Differential Accumulation of the APP CTFs and Reduction of Aβ peptides in *PS1* cKO Mice

(A) Western analysis of the APP CTFs in *PS1* cKO and littermate control mice. Western analysis was performed using lysate prepared from the cortex of cKO and littermate control mice (lanes 1–8) and CHO cells transfected with human wild-type *APP* cDNA (lane 11). The "Saeko" antiserum was used to detect the CTFs. At least five species of the CTFs were detected in the mouse brain (lanes 1–8), while one α-CTF (C83) and two β-CTF (C89 and C99) species were detected in the transfected CHO cells (lane 11). The two additional CTF bands were eliminated after treatment with potato acid phosphatase (lanes 9 and 10). The level of the CTFs is slightly higher in the cKO cortex at P18 (lane 2), and further increased at P22 (lane 4). The accumulation of the CTFs (C83 and C89) in the cKO cortex is very striking at the ages of 6 weeks (lane 6) and 6 months (lane 8), while the increase of the β-CTF (C99) is modest, compared to the control.

(B) Differential accumulation of the α- and β-CTFs in the cKO cortex. Brain lysate prepared from the cortex of *PS1* cKO mice at the age of 6 months was diluted as indicated (lanes 2–8), and immunoblotted with the "Saeko" antiserum along with the undiluted homogenate of the control cortex (lane 1). The level of the α-CTF (C83) and β-CTF (C89) in the cKO cortex is increased about 30-fold while the level of the β-CTF (C99) in the cKO cortex is increased about 3-fold relative to the control.

(C) Reduction of endogenous mouse Aβ40 and Aβ42 peptides in the cKO cortex. Relative levels of mouse Aβ40 and Aβ42 in the cortex of the cKO (n = 9) and control (n = 9) mice at the age of 3–6 months were determined by the BNT-77/BA27 and BNT-77/BC05 ELISA assays following immunodepletion of the APP CTFs using the "Saeko" antiserum, respectively. Levels of Aβ40 and Aβ42 in the cKO cortex are shown as relative values to that of the control, which are designated as 1.

(D) Reduction of human Aβ40 and Aβ42 peptides in the cKO cortex. The level of human Aβ40 and Aβ42 in the cortex of the cKO (n = 7) and control (n = 6) mice at the age of 6–9 weeks was measured by the 2G3/3D6 and 21F12/3D6 ELISA assays, respectively. In the control mice overexpressing human mutant APP, levels of human Aβ42 are slightly higher than that of Aβ40, most likely due to the Indiana mutation that is known to increase the production of Aβ42. In the cKO mice overexpressing human mutant APP, levels of both Aβ40 and Aβ42 are significantly reduced ($p < 0.01$, Student's t test). The reduction of Aβ40 (~42%) is more marked than that of Aβ42 (~27%) in the cKO cortex.

elimination of PS1 expression does not affect α- and β-secretase cleavages, these results indicate that PS1 is required for γ-secretase activity, and that lack of PS1 results in accumulation of γ-secretase substrates.

To investigate PS1 function in the generation of Aβ peptides in the adult cerebral cortex, we measured levels of Aβ40 and Aβ42 in the cortex of the cKO and the littermate control mice at the ages of 6 weeks and 6 months by enzyme-linked immunosorbent assay (ELISA). Well-characterized antibodies specific for Aβ40 and Aβ42—BA27 and BC05, respectively—were used for the assay (Duff et al., 1996; Suzuki et al., 1994). We found that levels of Aβ40 are reduced in the cortex of *PS1* cKO mice at both ages examined (Table 1). Surprisingly, we detected higher levels of Aβ42 in the cortex of cKO mice than in the control, and the increase becomes more substantial by the age of 6 months (Table 1). Given the pronounced age-dependent accumulation of the CTFs (as much as 30-fold by 6 months) in the cKO cortex, we then examined whether the antibodies used for ELISA detection, BA27 and BC05, crossreact with the CTFs by Western, IP-Western, and IP-ELISA. Western analysis showed that neither BA27 nor BC05 recognizes the high levels of the accumulated CTFs in the *PS1* cKO cortex (data not shown). Immunoprecipitation using either BA27 or BC05 followed by Western analysis, however, revealed that BC05 crossreacts with the APP CTFs, while BA27 does not, suggesting that levels of Aβ42

Table 1. Cortical Levels of Aβ40 and Aβ42 in the Control and cKO Mice

Genotype	Age	Aβ40 (pmol/g)	Aβ42 (pmol/g)
Control	6 weeks	1.67 ± 0.19	0.47 ± 0.09
cKO		0.92 ± 0.08	0.96 ± 0.08
(n = 4 ea.)			
Control	6 months	1.53 ± 0.28	0.49 ± 0.06
cKO		0.96 ± 0.15	1.29 ± 0.10
(n = 3 ea.)			

All values shown are mean ± SD. Levels of Aβ40 and Aβ42 were determined by the BNT-77/BA27 and BNT-77/BC05 ELISA assays, respectively. Similar changes in the level of Aβ40 and Aβ42 in the cKO and control mice were observed in three independent experiments.

Table 2. Relative Cortical Levels of Aβ40 and Aβ42 following CTF Immunodepletion (ID)

		Aβ40		Aβ42	
Genotype	Age (Months)	Control ID	ID	Control ID	ID
Control (n = 9)	3–6	1.00 ± 0.07	0.83 ± 0.06	1.00 ± 0.02	0.70 ± 0.02
cKO (n = 9)	3–6	0.46 ± 0.04[a]	0.23 ± 0.05[a]	1.66 ± 0.04[a]	0.53 ± 0.05[a]

All values (mean ± SEM) represent relative levels of Aβ40 and Aβ42 measured by the BNT-77/BA27 and BNT-77/BC05 ELISA assays, respectively, following immunodepletion with beads alone (Control ID) or with beads and the "Saeko" antiserum (ID). Similar changes in the level of Aβ40 and Aβ42 in the cKO and control mice were observed in three independent experiments.
[a] $p < 0.004$ compared to control by Mann Whitney test.

detected by BC05 may be artificially elevated in the cKO cortex due to the presence of high levels of the APP CTFs. To measure levels of Aβ40 and Aβ42 accurately, we removed the APP CTFs from the lysate by immunodepletion using the "Saeko" antiserum, and then determined the level of Aβ40 and Aβ42 in the supernatant by ELISA (Table 2). The complete removal of the CTFs in the supernatant was confirmed by Western analysis. Using this method, we found that the level of both Aβ40 and Aβ42 is reduced in the cKO cortex relative to the control (Table 2, Figure 4C). We recently generated cKO mice that overexpress the human mutant APP containing the Swedish and the Indiana (V717F) mutations (Mucke et al., 2000). The level of human Aβ40 and Aβ42 was determined by ELISA assays using antibodies that are specific for human Aβ40 and Aβ42 peptides and do not crossreact with APP CTFs (Johnson-Wood et al., 1997). We found that the level of human Aβ40 and Aβ42 is also reduced in the cKO cortex (Figure 4D). Together, our results showed that elimination of PS1 expression in most neurons of the adult mouse cerebral cortex markedly reduces the production of Aβ peptides, supporting the notion that targeting PS1 is an effective strategy for anti-amyloidogenic therapy in AD.

Normal Expression of Notch Downstream Effector Genes

Our previous studies of *PS1*$^{-/-}$ mice showed that PS1 is involved in the regulation of the Notch signaling pathway during neural development (Handler et al., 2000; Song et al., 1999). In the developing brain of both *PS1*$^{-/-}$ mice and *Notch1*$^{-/-}$ mice, the expression of the Notch downstream target gene *Hes5* is reduced and the expression of *Dll1* is increased, while *Hes1* expression is unaffected (de la Pompa et al., 1997; Handler et al., 2000). PS1 appears to regulate Notch signaling at the level of posttranslational activation since the level of Notch1 mRNA and protein is unchanged in the absence of PS1 (Handler et al., 2000). More specifically, PS1 is involved in the proteolytic production of NICD, based on the in vitro findings that NICD production is reduced in cultured *PS1*$^{-/-}$ cells transfected with truncated Notch1 constructs (De Strooper et al., 1999; Song et al., 1999). However, a direct in vivo assessment of PS1 function in NICD generation has not been possible because endogenous levels of NICD fall below the limits of detection with currently available methods. We therefore investigated PS1 function in Notch signaling in the adult cerebral cortex by examining expression of the Notch downstream target genes, *Hes1*, *Hes5*, and *Dll1*. Northern analysis of poly(A)$^+$ RNA derived from the cortex of cKO and littermate control mice at the age of 6 weeks showed similar levels of *Hes1*, *Hes5*, and *Dll1* expression (Figure 5). Quantitative comparison of the level of the *Hes1*, *Hes5*, and *Dll1* transcripts in the cortex of multiple mice (n = 4–5) from multiple experiments (n = 3) confirmed normal expression of these Notch downstream target genes in the cKO cortex. These re-

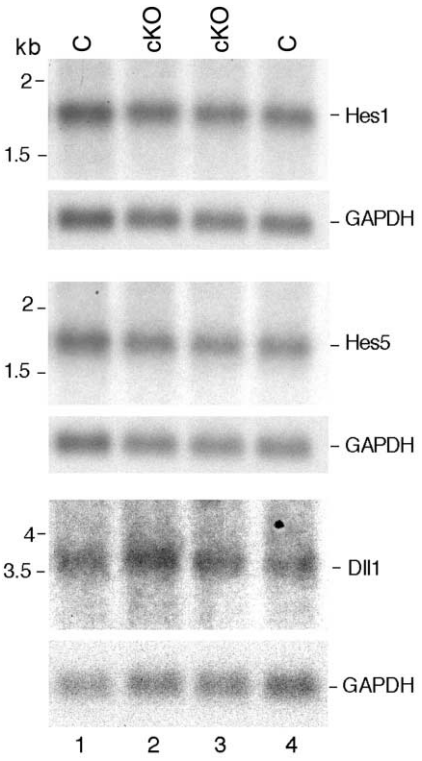

Figure 5. Unchanged Expression of *Hes1*, *Hes5*, and *Dll1* Transcripts in *PS1* cKO Mice

Northern analysis of *Hes1*, *Hes5*, and *Dll1* transcripts in *PS1* cKO and littermate control mice. Poly(A)$^+$ RNA was prepared from the cortex of cKO and control mice at the age of 6 weeks, and then hybridized with a *Hes1*, *Hes5*, or *Dll1* cDNA probe (Sasai et al., 1992; Takebayashi et al., 1995). The same blots were then hybridized with a control probe, *GAPDH*, to normalize the amounts of RNA in each lane. The level of each transcript was quantified using NIH Image software. Multiple experiments (n = 3) using poly(A)$^+$ RNA prepared from the cortex of cKO and control mice (n = 4–5) showed unchanged expression of *Hes1*, *Hes5*, and *Dll1* in the cKO cortex.

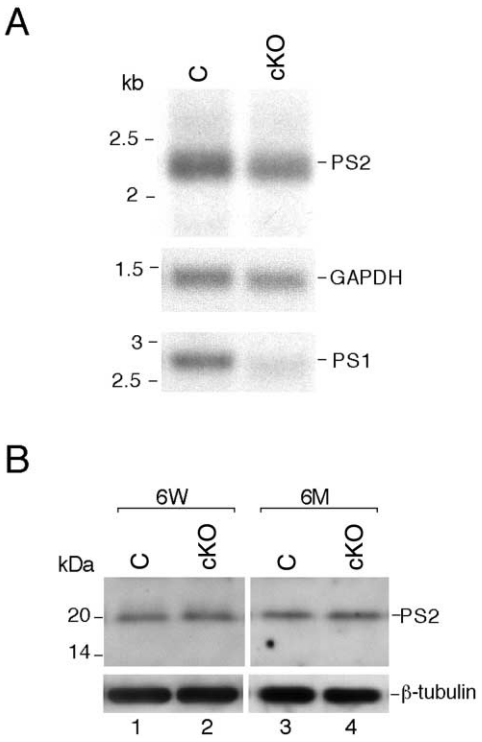

Figure 6. Unchanged Expression of PS2 in *PS1* cKO Mice

(A) Similar levels of *PS2* transcripts in *PS1* cKO and littermate control mice. Total RNA was prepared from the cortex of cKO and control mice at the age of 6 weeks, and then hybridized with a *PS2* cDNA probe. The same blot was then hybridized with a control probe, *GAPDH*, to normalize the amounts of RNA in each lane. (B) Similar levels of the PS2 CTF in *PS1* cKO and littermate control mice. Brain homogenate of the cortex of cKO and control mice at the age of 6 weeks was immunoblotted with the antiserum raised against the loop region of PS2 (Tomita et al., 1998). The same immunoblot was then incubated with the β-tubulin antibody to confirm similar amounts of total protein loaded in each lane.

sults demonstrate that the regulation of the Notch downstream effector genes differs in the embryonic and adult brain with respect to its dependence on PS1 function.

One possible explanation for the failure of PS1 inactivation to affect expression of Notch downstream genes in the adult brain could be a compensatory upregulation of presenilin-2 (PS2) expression. Alternatively, loss of PS1 could lead to an increase in the proteolytic processing of PS2 since the cleavage of PS proteins appears to be tightly regulated (Thinakaran et al., 1997; Tomita et al., 1997). To address these possibilities, we examined expression of PS2 by Northern and Western analyses. Northern analysis using total RNA derived from the cortex of *PS1* cKO and control mice at the age of 6 weeks showed no change in the level of *PS2* transcripts in the cKO cortex (Figure 6A). The level of the C-terminal fragment of PS2 is also unchanged in the cKO cortex (Figure 6B). These results indicate that elimination of PS1 function in the adult cortex does not result in a compensatory overproduction of PS2. It remains possible, however, that normal expression levels of PS2 in the adult cortex, which are higher than those in the embryonic brain relative to PS1, are sufficient to maintain the normal expression of the Notch downstream target genes. Alternatively, the regulation of Notch downstream genes in the adult brain might be independent of PS proteins.

Normal Synaptic Transmission and Plasticity in the Schaeffer Collateral Pathway

Our previous studies of *PS1*$^{-/-}$ mice revealed a critical role for PS1 in neurogenesis, neuronal differentiation, and migration during neural development, which is consistent with high levels of PS1 expression in the ventricular zone and the developing cortical plate (Handler et al., 2000; Shen et al., 1997). In the adult brain, PS1 is also expressed at relatively high levels in the hippocampus and neocortex (Figure 2C). To investigate whether PS1 is involved in the modulation of synaptic function in the adult brain, we examined the *PS1* cKO mice for deficits in synaptic transmission and plasticity in the Schaeffer collateral/commissural pathway of acute hippocampal slices.

We first evaluated the impact of PS1 inactivation on basal synaptic transmission. Input/output (I/O) curves were obtained by plotting the amplitude of the fiber volley (a measure of the number of recruited axons) versus the initial slope of the evoked field excitatory postsynaptic potential (fEPSP) response. As shown in Figure 7A, there is no significant difference in the I/O curve of the *PS1* cKO and control mice ($p > 0.5$, t test). In addition, the magnitude of the maximal response is similar in the cKO (1.286 ± 1.96 V/s) and in the control (1.376 ± 0.37 V/s). To assess possible effects on the presynaptic contribution to synaptic transmission, we next examined paired-pulse facilitation (PPF), a form of short-term plasticity. The cKO and control mice exhibited similar degrees of facilitation at all inter-stimulus intervals tested ($F_{7,259} = 0.280$; $p = 0.961$) (Figure 7B). These data indicate that basal synaptic transmission and short-term plasticity are normal in hippocampal area CA1 in the absence of PS1.

Subsequently, we examined the effect of PS1 inactivation on long-term potentiation (LTP) and long-term depression (LTD) in the CA1 region of the hippocampus, which are the best understood models of the synaptic modifications involved in learning and memory (reviewed in Bailey et al., 2000; Malenka and Nicoll, 1999). Previous studies have shown that LTP is enhanced in transgenic mice overexpressing FAD-linked mutant PS1 (Parent et al., 1999; Zaman et al., 2000). To determine whether PS1 plays a role in the initiation and maintenance of LTP, we induced LTP with theta burst stimulation (TBS) or a series of high frequency stimulation (HFS, 100 Hz tetanus). The magnitude of LTP induced by 5 TBS (measured 60 min after TBS) was essentially the same in the *PS1* cKO (144.9 ± 10) and in the control (148.5 ± 7.3; $p = 0.94$, t test) (Figure 7C). A series of HFS (three 100 Hz tetani), which is a stronger but less physiological LTP induction protocol (Baranes et al., 1998), produced a larger and longer lasting form of LTP. The magnitude of LTP, including the late phase of LTP measured 140 min after the last tetanus, was comparable in *PS1* cKO (167 ± 16) and control mice (148 ± 15; $p = 0.26$) (Figure 7D). LTD has been proposed to provide a complementary mechanism to LTP for the bidirectional

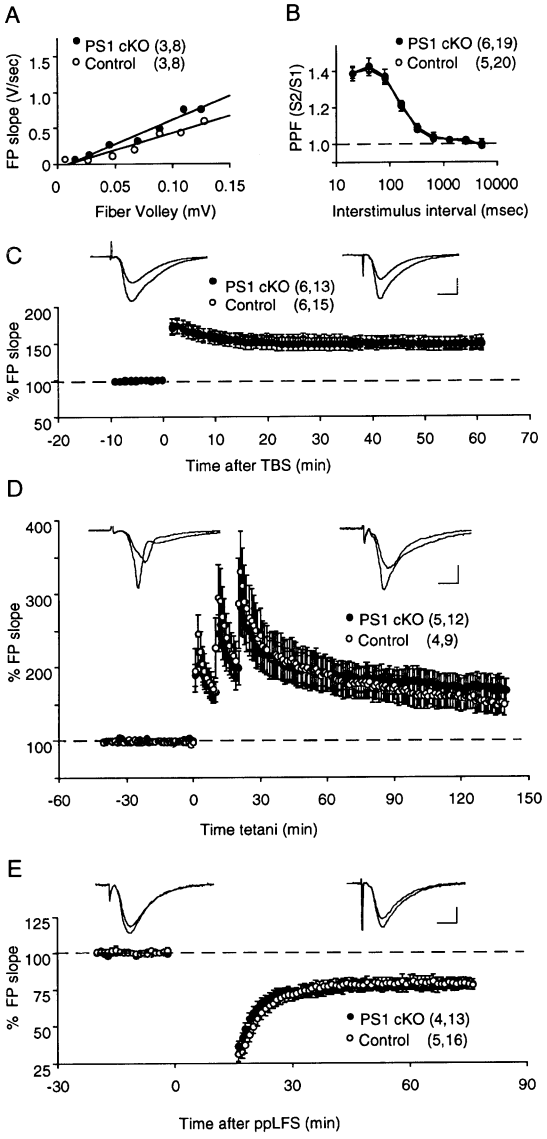

Figure 7. Normal Synaptic Transmission and Plasticity in Hippocampal Area CA1 of *PS1* cKO Mice

(A) Normal input/output curve of synaptic transmission in *PS1* cKO mice. The amplitude of the fiber volley (FV) is plotted against the initial slope of the evoked fEPSP for the cKO and littermate control mice. Each point represents data averaged across all slices for a narrow bin of FV amplitude. The lines represent the best linear regression fit (cKO: 6.6x-0.5, r2 = 0.97; control: 4.6x-0.04, r2 = 0.93).

(B) Normal paired pulse facilitation (PPF) in *PS1* cKO mice. The graph depicts the paired-pulse response ratio (2^{nd} fEPSP/1^{st} fEPSP) obtained at different interstimuls intervals (in m).

(C–E) Normal synaptic plasticity in *PS1* cKO mice. (C) Time course of the effects of 5 TBS on the fEPSP initial slope. Shown on top are examples of robust LTP induced in slices from control (left) and cKO (right) mice. Superimposed traces are averages of four consecutive responses recorded before (−1 min) and 60 min after TBS. (D) Normal late phase LTP induced by three tetanic trains (100 Hz, 1 s) in *PS1* cKO mice. The graph depicts the time course of the effects of three trains of HFS on the fEPSP initial slope. Traces on top, as in (C), were recorded before (−1 min) and 140 min after the first tetanus. (E) Normal LTD induced by paired-pulse low frequency stimulation (ppLFS) in *PS1* cKO mice. Time course of the effects of ppLFS on the fEPSP initial slope is shown. Traces on top, as in (C), were recorded before (−1 min) and 60 min after ppLFS. For all the panels, the results are expressed as average ± SEM. Filled circles represent *PS1* cKO and open circles represent controls. The number of mice (left) and slices (right) used in each experiment is indicated in parenthesis. Calibration bar: 0.5 mV, 5 ms.

modulation of synaptic efficacy (Bear, 1999). To investigate further whether PS1 plays a role in the modulation of synaptic plasticity in hippocampal area CA1, we induced LTD with a paired-pulse low frequency stimulation (ppLFS), a protocol effective in inducing LTD in slices from mature mice (Krezel et al., 1999). As shown in Figure 7E, the magnitude of LTD (measured 60 min after conditioning) was identical in the *PS1* cKO (78 ± 4) and the control (78 ± 4; p = 0.94) (Figure 7E). These results demonstrate that PS1 is not required for the induction and maintenance of LTP and LTD in the Schaeffer collateral pathway of the hippocampus.

Subtle Long-Term Spatial Memory Deficits in *PS1* cKO Mice

To assess the neuronal function of PS1 more globally, we used the Morris water maze task, a hippocampus-dependent paradigm for spatial learning and memory (Morris et al., 1982). During the acquisition phase of the task, mice learn the position of a hidden escape platform in a circular pool using distal spatial cues. Their performance is measured by the time required to locate the platform (escape latency) and by the distance traveled to reach the platform (path length). During the first 7 days of training, both groups of mice improved their performance at a similar rate, as indicated by the decreasing escape latencies and path lengths (Figures 8A and 8B). However, during the last 3 to 5 days of training, the control mice continued to improve while the performance of the cKO mice plateaued, resulting in significantly longer escape latencies and path lengths for the cKO group (Figures 8A and 8B). A two-way ANOVA showed a significant interaction effect of group x days ($F(9,261) = 2.06$; $p = 0.03$). Subsequent pairwise comparisons (Student's t tests) showed significantly longer latencies and path lengths for the cKO group versus the control group on days 8, 9, and 10 ($t(29)$; $p < 0.05$). Swimming speed and the degree of thigmotaxis (wall hugging) were similar in the cKO and control mice (data not shown), arguing against nonspecific effects due to impaired motor function and/or anxiety.

The *PS1* cKO and control mice were further tested in probe trials, in which the platform is removed from the pool, after 1, 5, and 10 days of training. If the mice have learned the position of the hidden platform using the distal cues, they tend to search preferentially in the quadrant (target quadrant) where the platform was previously located, and they swim across the precise platform location more frequently than the corresponding locations in other quadrants (platform crossings). After 1 and 5 days of training, the cKO and control mice showed no preference for the target quadrant (quadrant occupancy) and the platform location (platform crossing) relative to the remaining quadrants. After 10 days of training, both groups of mice searched preferentially in the target quadrant (Figures 8C and 8D). The total number of platform crossings by the cKO mice (2.27 ±

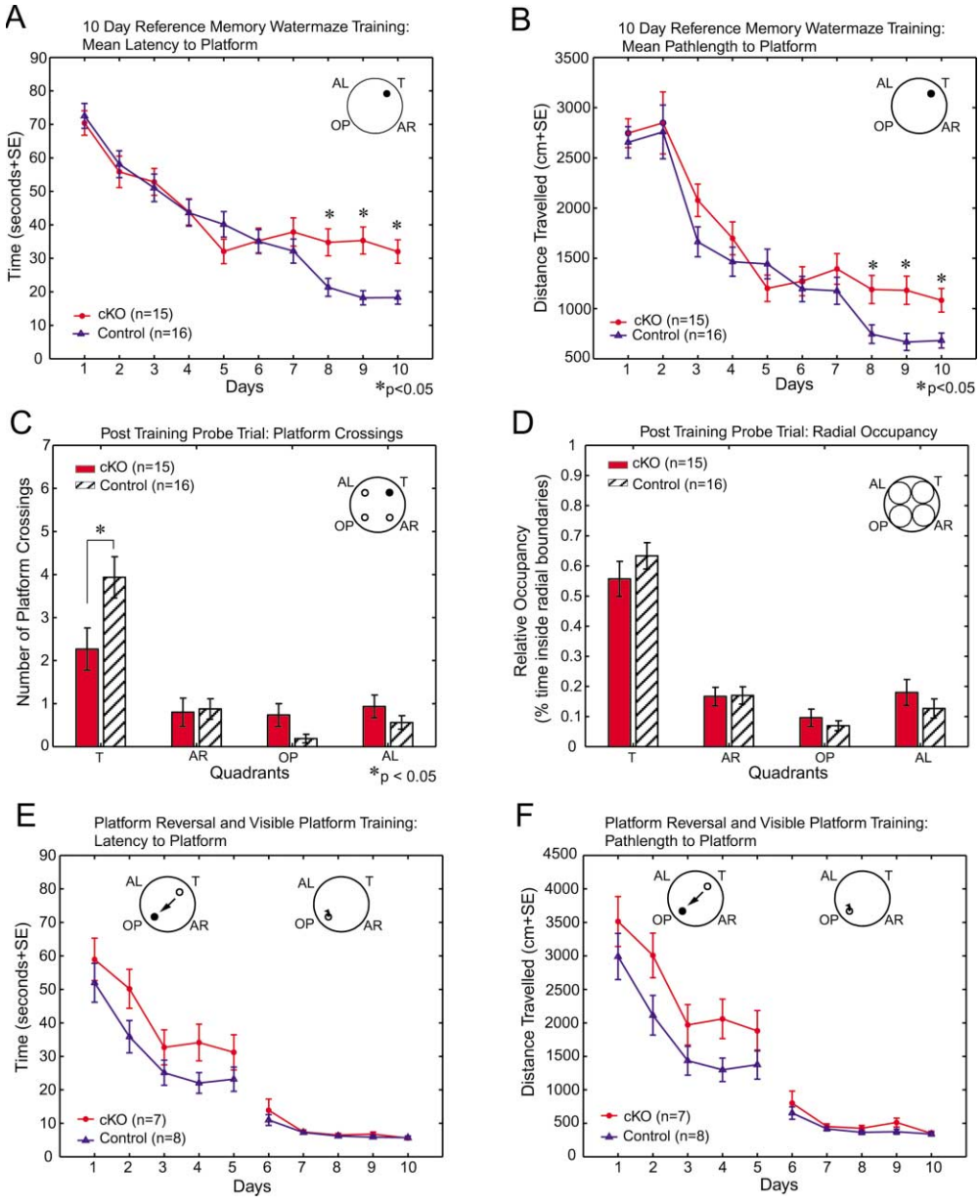

Figure 8. Mild Impairment of Spatial Learning and Memory in *PS1* cKO Mice

(A and B) Delayed escape latencies and longer path lengths exhibited by *PS1* cKO mice in the hidden platform version of the Morris water maze task. Escape latencies and path lengths of cKO and control mice over 10 days of training (four trials per day) were plotted. Both cKO and control mice learned similarly up to day 7, after which the cKO mice showed significantly longer latencies and path lengths (Student's t test, $p < 0.05$).

(C and D) Reduced platform crossings by *PS1* cKO mice in the probe trial after 10 days of training. Data were collected during the probe trial (90 s) immediately following the 10th day of training. The mean number of crossings through the target platform location was significantly lower in the cKO group (2.27 $\pm$ 0.49) than in the control group (3.94 $\pm$ 0.88) (Student's t test, $p < 0.05$). This difference indicates a subtle but significant deficit in the ability of the cKO mice to find the target using a higher spatial resolution strategy. However, radial quadrant occupancy, which is measured by the time spent in the target radial quadrant relative to the time spent in all four radial quadrants, was similar for cKO (0.557 $\pm$ 0.058) and controls (0.633 $\pm$ 0.044), indicating no significant difference in gross spatial navigation strategies between the two groups.

(E and F) Hidden platform reversal and visible platform tasks. Escape latencies and path lengths of cKO and control mice over 5 days of training (four trials per day) in the platform-reversal phase of the hidden platform water maze task were plotted. The cKO mice showed longer latencies and path lengths, particularly on days 2 and 4 ($p < 0.05$). The platform-reversal phase was followed by a 5 day visible platform version of the task. Both the cKO and control mice performed extremely well with indistinguishable latencies of $\sim$5 s and path lengths of $\sim$350 cm. This result indicates that the cKO mice do not exhibit a general motivational or physical deficit in swimming performance to the target location. For all the panels, the results are expressed as average $\pm$ SEM. Filled circles represent *PS1* cKO, and triangles represent controls. Abbreviations: T, target quadrant; OP, opposite quadrant; AL, adjacent left quadrant; AR, adjacent right quadrant.

0.49), however, was significantly lower than that of the control mice (3.94 ± 0.88; $p < 0.05$), though the target radial quadrant occupancies of cKO (0.557 ± 0.058) and control (0.633 ± 0.044) mice were similar ($p = 0.3$) (Figures 8C and 8D).

We then moved the hidden platform to a different location in the opposite quadrant of the pool (platform-reversal phase), and repeated the acquisition experiment for 5 more days. The displacement of the platform resulted in an initial increase in the mean escape latency and path length of both groups of mice (Figures 8E and 8F). The cKO mice again exhibited poorer performance than the controls with longer escape latencies and path lengths (e.g., $p < 0.05$ at day 4) (Figures 8E and 8F). To determine whether the delayed escape latencies of the cKO mice might be caused by deficits in motivation, sensory, and/or motor abilities, both groups of mice were also tested in the visible platform version of the task. The escape latencies and path lengths of the cKO and control mice were very low and essentially indistinguishable (Figures 8E and 8F). Taken together, these results demonstrate a mild but specific impairment in spatial learning and memory in the *PS1* cKO mice.

Discussion

Recent studies using *PS1*$^{-/-}$ cells and transition state analog inhibitors provided strong evidence that PS1 is required for γ-secretase activity (De Strooper et al., 1998; Esler et al., 2000; Li et al., 2000). It is therefore critically important to test the feasibility of targeting PS1 for anti-amyloidogenic therapies in vivo. Although germline *PS1* inactivation has been shown to reduce the production of Aβ peptides markedly in cultured embryonic neurons, a requirement for PS1 in Aβ generation in the adult cerebral cortex remained to be demonstrated. Furthermore, our previous studies showed that PS1 is required for neurogenesis and Notch downstream target genes during brain development (Handler et al., 2000; Shen et al., 1997), but it remained unclear whether PS1 played a similar role in the regulation of Notch downstream target genes in the adult brain.

To address these questions, we developed a conditional *PS1* KO mouse, in which expression of *PS1* is selectively eliminated in most neurons of the cerebral cortex beginning at postnatal day 18 (Figure 2). Here we show that the adult cerebral cortex of the *PS1* cKO mouse is morphologically normal, in contrast to the pleiotropic phenotypes associated with PS1 deficiency in the embryonic brain. Despite the differential effects of PS1 inactivation in the embryonic and adult brain, the role of PS1 in the generation of Aβ peptides appears similar. Consistent with previous studies using cultured *PS1*$^{-/-}$ neurons (De Strooper et al., 1998), we found a substantial reduction in the level of both mouse and human Aβ40 and Aβ42 in the adult cortex of *PS1* cKO mice (Table1, Figures 4C and 4D). This result provides important in vivo confirmation of the requirement for PS1 in the generation of Aβ peptides in the adult cerebral cortex, where accumulation and deposition of Aβ peptides are important and invariant features of AD. Interestingly, the reduction of Aβ40 is more significant than that of Aβ42 in the cKO mice, raising the possibility that PS2 may play a more important role in the production of Aβ42. Recent studies using embryonic stem cells derived from *PS1*$^{-/-}$;*PS2*$^{-/-}$ mice showed that in the absence of both presenilins, the level of Aβ peptides was undetectable (Herreman et al., 2000; Zhang et al., 2000). We plan to investigate whether the generation of Aβ peptides is abolished completely in the adult cerebral cortex of *PS1* cKO mice in the *PS2*$^{-/-}$ background.

The most striking feature of the disrupted APP processing is the 30-fold accumulation of the APP CTFs in *PS1* cKO mice by the age of 6 months (Figure 4). Interestingly, the APP β-CTFs (C89 and C99) accumulate differentially in the absence of PS1, with the increase in the level of C89 and C99 measuring approximately 30- and 3-fold, respectively (Figure 4). The levels of the α-CTF (C83) are also elevated by as much as 30-fold (Figure 4). Since the CTFs represent the substrates for γ-secretase cleavage, these results are consistent with a requirement of PS1 for γ-secretase activity. The differential accumulation of the CTFs, particularly C89 and C99, which are cleavage products of β-secretase, is likely due to the differences in their half lives. Alternatively, C99 could be converted to C89 by β-secretase, resulting in much lower levels of C99 relative to C89 in the cKO mice. Furthermore, we found that all APP CTFs are present in phosphorylated and nonphosphorylated forms in the brain of both control and cKO mice (Figure 4 and data not shown). The cytoplasmic domain of full-length APP has been shown to be phosphorylated in cultured neurons and adult rat brain by cdk5 on Thr668, which resides in the C-terminal region common to all APP CTF species (Iijima et al., 2000; Oishi et al., 1997). This phosphorylation event may therefore account for the observed phosphorylation of the CTFs. Although the physiological significance of APP phosphorylation is unclear, there is evidence suggesting that it may be associated with the regulation of Aβ generation and neurite extension (Ando et al., 1999; Buxbaum et al., 1993).

Identification of the close association between PS1 and the γ-secretase activity has sparked interest in the use of PS1 as a therapeutic target in AD. The critical role of PS1 in Notch signaling during neural development, however, raised the possibility that inhibition of PS1 function in the adult brain might be deleterious. In contrast to the reduction of Notch1 activity in the *PS1*$^{-/-}$ embryonic brain, as evidenced by reduced expression of *Hes5* and increased expression of *Dll1*, expression of the Notch1 downstream effector genes *Hes1*, *Hes5*, and *Dll1* is unchanged in the cortex of *PS1* cKO mice (Figure 5). It is possible that expression of PS2 in the adult cortex, which is relatively high compared to its expression in the embryonic brain, is sufficient to maintain normal expression of these Notch downstream genes. Alternatively, it is also possible that the regulation of expression of these genes in the adult brain differs from that in the embryonic brain and is independent of presenilins.

A recent report showed that the *C. elegans* PS1 homologs, sel-12 and hop-1, are required for the proper morphology and function of cholinergic interneurons (Wittenburg et al., 2000). To investigate whether PS1 plays a role in the regulation of synaptic function in the mammalian nervous system, we studied the *PS1* cKO mice for

subtle behavioral abnormalities and deficits in synaptic transmission and plasticity. Thorough examination of the cKO and littermate control mice failed to identify any significant deficits in basal synaptic transmission and plasticity in the Schaeffer collateral pathway of the hippocampus (Figure 7). However, the Morris water maze task revealed a mild delayed deficit in spatial learning and memory in the *PS1* cKO mice (Figure 8). Although the performance of the cKO mice during initial stages of learning was not significantly different from that of the control mice, the performance of the cKO mice plateaued during the later stages of this reference memory task, while the control mice continued to improve (Figure 8). In addition, the platform crossings of the cKO mice were much lower than the control in the probe trial after 10 days of training, but the target quadrant occupancy was similar in both groups of mice. The cKO mice are thus able to learn the general location of the platform, but with less spatial precision than the control mice. These findings suggest a deficit in detailed spatial navigation in the cKO mice, though gross spatial navigation is normal.

The platform-reversal phase of the task also elicited a poorer performance by the cKO mice in the escape latencies and path length from the first training day, indicating a mild learning deficit (Figure 8). The identical performance by the cKO and control mice in the visible platform task indicates that the deficits exhibited by the cKO are due to spatial learning and memory rather than a visual, motor, or motivational impairment. Elimination of PS1 expression in the adult cortex thus leads to subtle but significant deficits in learning and memory, indicating a requirement for PS1 in normal neuronal function. The normal synaptic transmission and plasticity in the Schaeffer collateral pathway in the cKO mice, however, suggest that the observed cognitive impairment may be mediated by selective abnormalities in other hippocampal or cortical circuits. It will be interesting to determine whether the absence of both presenilins will evoke more severe impairments in learning and memory.

Although loss of PS1 function did not lead to impaired synaptic transmission and plasticity in the Schaeffer collateral pathway, previous studies indicated that overexpression of FAD-linked mutant PS1, but not wild-type PS1, in transgenic mice results in enhanced LTP in this pathway (Parent et al., 1999; Zaman et al., 2000). It is unclear whether the enhancement of LTP in these transgenic mice influences their behavior, but the present results suggest that altered PS1 activity can produce alterations in learning and memory. The mechanism by which PS1 may regulate synaptic function is unknown. Recent reports have shown that the C-terminal region of PS1 interacts with PDZ domain-containing proteins, including X11α and X11β (Lau et al., 2000; Tomita et al., 1999; Xu et al., 1999). X11 proteins form a complex with Munc18-1 in the brain, which is essential for synaptic vesicle exocytosis (Borg et al., 1998; Okamoto and Sudhof, 1997; Verhage et al., 2000). In addition, X11α is part of an evolutionarily conserved heterotrimeric complex CASK/X11α/Veli, which is thought to be involved in coupling synaptic vesicle exocytosis and neuronal cell adhesion (Borg et al., 1998, 1999; Butz et al., 1998). Alternatively, PS1 may be involved in synaptic function indirectly through its role in APP processing. An interaction has been reported between the cytoplasmic YENPTY motif of APP and the PTB domain of X11α (Borg et al., 1996; Zhang et al., 1997). Although the normal physiological role of APP in the interaction of X11α and Munc18-1 and the formation of the CASK/X11α/Veli complex is unclear, the striking accumulation of the APP CTFs in the cortex of *PS1* cKO mice may disrupt these complexes and lead to deficits in synaptic function.

In summary, our analysis of the *PS1* cKO mice provides direct in vivo evidence of the requirement for PS1 in normal APP processing and the generation of amyloid peptides. Surprisingly, the regulation of the Notch downstream genes in the adult brain is independent of PS1, in contrast to the regulation of Notch activity by PS1 during brain development. It is therefore likely that therapeutic γ-secretase inhibitors will be able to achieve reduced production of Aβ peptides in the adult brain without unwanted side effects on the expression of the Notch target genes. PS1 also appears to be required for normal neuronal function in the adult brain, but the observed cognitive deficits in the *PS1* cKO mice are relatively subtle and may be restricted to specific neural circuits. In support of this notion, synaptic transmission and plasticity in hippocampal area CA1 of the cKO mice was entirely normal. It will be important, however, to determine whether mice lacking both presenilins exhibit any additional abnormalities since therapeutic γ-secretase inhibitors are likely to inhibit both PS1- and PS2-mediated activities. Based on our current study, the benefits of therapeutic γ-secretase inhibitors may outweigh the potentially detrimental effects associated with targeting PS1 function.

Experimental Procedures

Generation of Floxed *PS1*, *CaMKII-Cre,* and *PS1* cKO Mice

The targeting vector was transfected into J1 (129/Sv) ES cells, and the ES cells carrying the modified *PS1*, *fPS1*, and *PS1*$^{\Delta}$ allele were generated as described in Yu et al., 2000. The ES cells carrying the *fPS1* or the *PS1*$^{\Delta}$ allele were injected into mouse blastocysts to generate chimeric mice, which were bred to C57BL/6J to generate heterozygous *fPS1* and *PS1*$^{\Delta}$ mice, respectively. The construction of the α*CaMKII-Cre* transgene was similar to that described in Mayford et al., 1996. The α*CaMKII* promoter segment contains $\sim$8.5 kb genomic DNA upstream of the transcription initiation site of the α*CaMKII* gene and 84 bp of the 5′ noncoding exon, which is followed by a hybrid intron, *Cre* cDNA, and the SV40 polyadenylation signal. The α*CaMKII-Cre* (*CaM-Cre*) transgene was injected into the pronucleus of C57BL/6J and CBA hybrid embryos. The transgenic mice were then backcrossed several generations to C57BL/6J. The *fPS1* mice were bred to *CaM-Cre* transgenic mice to obtain *PS1* cKO (*fPS1/fPS1;CaM-Cre* or *PS1*$^{\Delta}$*/fPS1;CaM-Cre*) and littermate control (*fPS1/fPS1* or *PS1*$^{\Delta}$*/fPS1*) mice used in the study.

In Situ Hybridization

A 260 bp sense or antisense riboprobe specific for *PS1* exons 2 and 3 was synthesized using an in vitro transcription kit (Boehringer Mannheim). In situ hybridization was carried out as previously described (Schaeren-Wiemers and Gerfin-Moser, 1993).

Western and IP-Western

The αPS1Loop antiserum (1:10,000) was raised against amino acid residues 320–375 of human PS1, and recognizes both human and mouse PS1 (Thinakaran et al., 1996). The PS2 antiserum (1:1000), G2L, was raised against a GST-PS2loop (301–361) fusion protein (Tomita et al., 1998). The following APP antibodies were used: polyclonal C7 (residues 676–695) (Knops et al., 1995); C-terminal polyclonal "Saeko" (1:10,000) (Kawarabayashi et al., 1996); monoclonal

192 (0.25 μg/ml), which specifically recognizes the C terminus of β-APPs (Knops et al., 1995); polyclonal 1736 antisera raised against N-terminal of Aβ (residues 595–611) (Haass et al., 1992); and monoclonal antibody 22C11 (0.15 μ/ml; Roche), which recognizes an N-terminal epitope (residues 66–81) of APP.

Mouse cortex was dissected on ice and homogenized in cold lysis buffer (50 mM Tris HCl, pH 7.4, 150 mM NaCl, 1% NP-40, 2 mM EDTA, protease inhibitors). Protein extracts (40 μg) of cKO and control cortex were separated on 4%–12%, 4%–20% Tris-Glycine (Invitrogen) or 16% Tris-tricine SDS-PAGE, and transferred to PVDF membrane. The blots were incubated with appropriate primary antibody and developed with enhanced chemiluminescence (ECL Plus, Amersham). For Western blotting, the same blot was also incubated with anti-tubulin antibody to normalize the amounts of total protein loaded in each lane.

ELISA Assays

For the detection of mouse endogenous Aβ peptides, the cortex of cKO and control mice was dissected on ice, and then homogenized in RIPA buffer containing complete protease inhibitors. The samples were analyzed using the BNT-77/BA27 and BNT-77/BC05 quantitative sandwich ELISA assays (Duff et al., 1996) to determine the level of Aβ40 and Aβ42, respectively. Levels of the human Aβ40 and Aβ42 peptides in the cortex of cKO and control mice that overexpress the human mutant APP transgene were measured by the 2G3/3D6 and 21F12/3D6 ELISA assays, respectively, as previously described (Johnson-Wood et al., 1997). The experimenters were blind to the genotypes of the samples.

Electrophysiology

Hippocampal slices (400 μm) from cKO and littermate control mice (aged 3–6 months) were prepared as described (Kirkwood et al., 1999). The slices were maintained in an interface storage chamber containing artificial cerebrospinal fluid (ACSF) at 30°C for at least an hour prior to recording. Stimulation (200 μs) pulses were delivered with a bipolar concentric metal electrode. Synaptic strength was quantified as the initial slope of field potentials recorded with ACSF filled microelectrodes (1 to 2 MΩ). Baseline responses were collected at 0.07 Hz with a stimulation intensity that yielded a half-maximal response. Two conditioning protocols were used to induce LTP. One was five episodes of theta burst stimulation (TBS) delivered at 0.1 Hz. TBS consisted of ten stimulus trains delivered at 5–7 Hz; each train consisted of four pulses at 100 Hz. The other protocol was three 100 Hz tetani delivered every 10 min. LTD was induced with 900 paired-pulses (40 ms apart) delivered at 1 Hz. Average responses (± SEM) are expressed as percent of pre-TBS baseline response (at least 10 min of stable responses). A repeated measures ANOVA and nonpaired t test were used to asses statistical significance. The experimenters were blind to the genotypes of the mice.

Morris Water Maze Task

The water maze is a circular pool 160 cm in diameter. Mouse position in the maze was tracked by a ceiling mounted Dragon Tracker system (60 Hz) connected to a computer. Position information was analyzed by custom Matlab software (Linus Sun and Bogdan Fedeles). Mice were housed in a standard 12 hr light-dark cycle and were tested at 2 p.m. every day. Each mouse was given four trials daily with a maximum duration of 90 s separated by a minimum of 15 min. If mice did not find the hidden platform, they were guided to the platform and allowed to remain on it for 15 s. Two groups of mice at the ages of 5 or 8 months (∼eight mice per genotype per age group) were trained in the hidden platform task for 10 or 12 days, respectively. Similar results were obtained from these two independent experiments, and so the data were combined. After 1, 5, and 10 days of training, the hidden platform was removed and a 90 s probe trial was performed on both age groups. After 12 days of training in the hidden platform task, the platform was transferred to the corresponding location of the opposite quadrant (reversal of platform), and the older groups of mice (8 months, N = 7,8) were trained with four trials daily for 5 days to locate the new platform position. The same groups of mice were further tested for 5 days in the visible platform task, where a proximal cue was added to the reversed platform position. The experimenters were blind to the genotypes of the mice.

Acknowledgments

The authors would like to thank Wen Cheng and Eddie Meloni for technical assistance, Dennis Selkoe and Bing Zheng for APP antibodies and ELISA measurements of human Aβ peptides, Lennart Mucke for the APP transgenic mice, Mikio Shoji for the "Saeko" antiserum, Gopal Thinakaran for PS1 and Takeshi Iwatsubo for PS2 antisera, Peter St. George-Hyslop for PS2, and Ryoichiro Kageyama for Hes1, Hes5, and Dll1 plasmids. This work was supported in part by grants from NIH and Alzheimer's Association.

Received August 14, 2000; revised June 12, 2001.

References

Ando, K., Oishi, M., Takeda, S., Iijima, K., Isohara, T., Nairn, A., Kirino, Y., Greengard, P., and Suzuki, T. (1999). Role of phosphorylation of Alzheimer's amyloid precursor protein during neuronal differentiation. J. Neurosci. *19*, 4421–4427.

Bailey, C.H., Giustetto, M., Huang, Y.Y., Hawkins, R.D., and Kandel, E.R. (2000). Is heterosynaptic modulation essential for stabilizing Hebbian plasticity and memory? Nat. Rev. Neurosci. *1*, 11–20.

Baranes, D., Lederfein, D., Huang, Y.Y., Chen, M., Bailey, C.H., and Kandel, E.R. (1998). Tissue plasminogen activator contributes to the late phase of LTP and to synaptic growth in the hippocampal mossy fiber pathway. Neuron *21*, 813–825.

Bear, M.F. (1999). Homosynaptic long-term depression: a mechanism for memory? Proc. Natl. Acad. Sci. USA *96*, 9457–9458.

Borg, J., Straight, S., Kaech, S., De Taddeo-Borg, M., Droon, D., Karnak, D., Turner, R., Kim, S., and Margolis, B. (1998). Identification of an evolutionarily conserved heterotrimeric protein complex involved in protein targeting. J. Biol. Chem. *273*, 31633–31636.

Borg, J., Lopez-Figueroa, M., De Taddeo-Borg, M., Kroon, D., Turner, R., Watson, S., and Margolis, B. (1999). Molecular analysis of the X11-mLin-2/CASK complex in brain. J. Neurosci. *19*, 1307–1316.

Borg, J.P., Ooi, J., Levy, E., and Margolis, B. (1996). The phosphotyrosine interaction domains of X11 and FE65 bind to distinct sites on the YENPTY motif of amyloid precursor protein. Mol. Cell. Biol. *16*, 6229–6241.

Butz, S., Okamoto, M., and Sudhof, T. (1998). A tripartite protein complex with the potential to couple synaptic vesicle exocytosis to cell adhesion in brain. Cell *94*, 773–782.

Buxbaum, J.D., Koo, E.H., and Greengard, P. (1993). Protein phosphorylation inhibits production of Alzheimer amyloid beta/A4 peptide. Proc. Natl. Acad. Sci. USA *90*, 9195–9198.

Buxbaum, J., Thinakaran, G., koliatsos, V., O'Callahan, J., Slunt, H., Price, D., and Sisodia, S. (1998). Alzheimer amyloid protein precursor in the rat hippocampus transport and processing through the perforant path. J. Neurosci. *18*, 9629–9637.

Cai, H., Wang, Y., McCarthy, D., Wen, H., Borchelt, D., Price, D., and Wong, P. (2001). BACE1 is the major b-secretase for generation of Ab peptides by neurons. Nat. Neurosci. *4*, 233–234.

de la Pompa, J.L., Wakeham, A., Correia, K.M., Samper, E., Brown, S., Aguilera, R.J., Nakano, T., Honjo, T., Mak, T.W., Rossant, J., and Conlon, R.A. (1997). Conservation of the Notch signalling pathway in mammalian neurogenesis. Development *124*, 1139–1148.

De Strooper, B., Saftig, P., Craessaerts, K., Vanderstichele, H., Guhde, G., Annaert, W., Von Figura, K., and Van Leuven, F. (1998). Deficiency of presenilin-1 inhibits the normal cleavage of amyloid precursor protein. Nature *391*, 387–390.

De Strooper, B., Annaert, W., Cupers, P., Saftig, P., Craessaerts, K., Mumm, J.S., Schroeter, E.H., Schrijvers, V., Wolfe, M.S., Ray, W.J., et al. (1999). A presenilin-1-dependent gamma-secretase-like protease mediates release of Notch intracellular domain. Nature *398*, 518–522.

Duff, K., Eckman, C., Zehr, C., Yu, X., Prada, C.-M., Perez-Tur, J., Hutton, M., Buee, L., Harigaya, Y., Yager, D., et al. (1996). Increased

amyloid-β42(43) in brains of mice expressing mutant presenilin 1. Nature *383*, 710–713.

Esler, W., Kimberly, W., Ostaszewski, B., Diehl, T., Moore, C., Tsai, J.-Y., Rahmati, T., Xia, W., Selkoe, D., and Wolfe, M. (2000). Transition-state analogue inhibitors of γ-secretase bind directly to presenilin-1. Nat. Cell Biol. *2*, 428–434.

Haass, C., Schlossmacher, M.G., Hung, A.Y., Vigo-Pelfrey, C., Mellon, A., Ostaszewski, B.L., Lieberburg, I., Koo, E.H., Schenk, D., Teplow, D.B., and Selkoe, D.J. (1992). Amyloid β-peptide is produced by cultured cells during normal metabolism. Nature *359*, 322–325.

Handler, M., Yang, X., and Shen, J. (2000). Presenilin-1 regulates neuronal differentiation during neurogenesis. Development *127*, 2593–2606.

Herreman, A., Serneels, L., Annaert, W., Collen, D., Schoonjans, L., and De Strooper, B. (2000). Total inactivation of γ-secretase activity in presenilin-deficient embryonic stem cells. Nat. Cell Biol. *2*, 461–462.

Iijima, K., Ando, K., Takeda, S., Satoh, Y., Seki, T., Itahara, S., Greengard, P., Kirino, Y., Nairn, A., and Suzuki, T. (2000). Neuron-specific phosphorylation of Alzheimer's β-amyloid precursor protein by cyclin-dependent kinase 5. J. Neurochem. *75*, 1085–1091.

Jarrett, J.T., Berger, E.P., and Lansbury, P.T., Jr. (1993). The carboxy terminus of the beta amyloid protein is critical for the seeding of amyloid formation: Implications for the pathogenesis of Alzheimer's disease. Biochemistry *32*, 4693–4697.

Johnson-Wood, K., Lee, M., Motter, R., Hu, K., Gordon, G., Barbour, R., Khan, K., Gordon, M., Tan, H., Games, D., Lieberburg, I., Schenk, D., Seubert, P., and MConlogue, L. (1997). Amyloid precursor protein processing and Aβ42 deposition in a transgenic mouse model of Alzheimer disease. Proc. Natl. Acad. Sci. USA *94*, 1550–1555.

Kawarabayashi, T., Shoji, M., Sato, M., Sasaki, A., Ho, L., Eckman, C.B., Prada, C.M., Younkin, S.G., Kobayashi, T., Tada, N., et al. (1996). Accumulation of beta-amyloid fibrils in pancreas of transgenic mice. Neurobiol. Aging *17*, 215–222.

Kirkwood, A., Rozas, C., Kirkwood, J., Perez, F., and Bear, M.F. (1999). Modulation of long-term synaptic depression in visual cortex by acetylcholine and norepinephrine. J. Neurosci. *19*, 1599–1609.

Knops, J., Suomensaari, S., Lee, M., McConlogue, L., Seubert, P., and Sinha, S. (1995). Cell-type and amyloid precursor protein-type specific inhibition of a beta release by Bafilomycin A1, a selective inhibitor of vacuolar ATPases. J. Biol. Chem. *270*, 2419–2422.

Krezel, W., Giese, K.P., Silva, A.J., and Chapman, P.F. (1999). Long-term depression is unpaired in hippcampus of adult a-CAMKIIT286A. Abstr. Soc. Neurosci. *25*, 987.

Lah, J.J., Heilman, C.J., Nash, N.R., Rees, H.D., Yi, H., Counts, S.E., and Levey, A.I. (1997). Light and electron microscopic localization of presenilin1 in primate brain. J. Neurosci. *17*, 1971–1980.

Lau, K., McLoughlin, D., Standen, C., and Miller, C. (2000). X11a and X11b interact with presenilin-1 via their PDZ domains. Mol. Cell. Neurosci. *16*, 557–565.

Li, Y.-M., Xu, M., Lai, M.-T., Huang, Q., Castro, J., DiMuzio-Mower, J., Harrison, T., Lellis, C., Nadin, A., Neduvelil, J., Register, R., Sardana, M., Shearman, M., Smith, A., Shi, X.-P., Yin, K.-C., Shafer, J., and Gardell, S. (2000). Photoactivated γ-secretase inhibitors directed to the active site covalently label presenilin 1. Nature *405*, 689–694.

Luo, Y., Bolon, B., Kahn, S., Bennett, B., Babu-khan, S., Denis, P., Fan, W., Kha, H., Zhang, J., Gong, Y., et al. (2001). Mice deficient in BACE1, the Alzheimer's b-secretase, have normal phenotype and abolished b-amyloid generation. Nat. Neurosci. *4*, 231–232.

Malenka, R.C., and Nicoll, R.A. (1999). Long-term potentiation—a decade of progress? Science *285*, 1870–1874.

Mayford, M., Bach, M.E., Huang, Y., Wang, L., Hawkins, R.C., and Kandel, E. (1996). Control of memory formation through regulated expression of a CaMKII transgene. Science *274*, 1678–1683.

Minichiello, L., Korte, M., Wolfer, D., Kuhn, R., Unsicker, K., Cestari, V., Rossi-Arnaud, C., Lipp, H., Bonhoeffer, T., and Klein, R. (1999). Essential role of TrkB receptors in hippocampus-mediated learning. Neuron *24*, 401–414.

Morris, R., Garrud, P., Rowlins, J., and O'Keefe, J. (1982). Place navigation impaired in rats with hippocampal lesions. Nature *297*, 681–683.

Mucke, L., Masliah, E., Yu, G.O., Mallory, M., Rockenstein, E., Tatsuno, G., Hu, K., Kholodenko, D., Johnson-Wood, K., and McConlogue, L. (2000). High-level neuronal expression of Ab1–42 in wild-type human amyloid protine precursor transgenic mice: synaptotoxicity without plaque formation. J. Neurosci. *20*, 4050–4058.

Oishi, M., Nairn, A., Czernik, A., Lim, G., Isohara, T., Gandy, S., Greengard, P., and Suzuki, T. (1997). The cytoplasmic domain of Alzheimer's amyloid precursor protein is phosphorylated at Thr654, Ser655, and Thr668 in adult brain and cultured cells. Mol. Med. *3*, 111–123.

Okamoto, M., and Sudhof, T. (1997). Mints, Munc18-interacting proteins in synaptic vesicle exocytosis. J. Biol. Chem. *272*, 31459–31464.

Parent, A., Linden, D., Sisodia, S., and Borchelt, D. (1999). Synaptic transmission and hippocampal long-term potentiation in transgenic mice expressing FAD-linked presenilin 1. Neurobiol. Dis. *6*, 56–62.

Sasai, Y., Kageyama, R., Tagawa, Y., Shigemoto, R., and Nakanishi, S. (1992). Two mammalian helix-loop-helix factors structurally related to *Drosophila hairy* and *Enhancer of split*. Genes Dev. *6*, 2620–2634.

Schaeren-Wiemers, N., and Gerfin-Moser, A. (1993). A single protocol to detect transcripts of various types and expression levels in neural tissue and cultured cells: *in situ* hybridization using digoxigenin-labelled cRNA probes. Hisotchemistry *100*, 431–440.

Scheuner, D., Eckman, C., Jensen, M., Song, X., Citron, M., Suzuki, N., Bird, T.D., Hardy, J., Hutton, M., Kukull, W., et al. (1996). Secreted amyloid β protein similar to that in the senile plaques of Alzheimer's disease is increased *in vivo* by the presenilin 1 and 2 and *APP* mutations linked to familial Alzheimer's disease. Nat. Med. *2*, 864–870.

Shen, J., Bronson, R.T., Chen, D.F., Xia, W., Selkoe, D.J., and Tonegawa, S. (1997). Skeletal and CNS defects in presnilin-1 deficient mice. Cell *89*, 629–639.

Simons, M., de Strooper, B., Multhaup, G., Tienari, P.J., Dotti, C.G., and Beyreuther, K. (1996). Amyloidogenic processing of the human amyloid precursor protein in primary cultures of rat hippocampal neurons. J. Neurosci. *16*, 899–908.

Song, W., Nadeau, P., Yuan, M., Yang, X., Shen, J., and Yankner, B.A. (1999). Proteolytic release and nuclear translocation of Notch-1 are induced by presenilin-1 and impaired by pathogenic presenilin-1 mutations. Proc. Natl. Acad. Sci. USA *96*, 6959–6963.

Suzuki, N., Iwatsubo, T., Odaka, A., Ishibashi, Y., Kitada, C., and Ihara, Y. (1994). High tissue content of soluble β1–40 is linked to cerebral amyloid angiopathy. Am. J. Pathol. *145*, 452–460.

Takebayashi, K., Akazawa, C., Nakanishi, S., and Kageyama, R. (1995). Structure and promoter analysis of the gene encoding the mouse helix-loop-helix factor HES-5. Identification of the neural precursor cell-specific promoter element. J. Biol. Chem. *270*, 1342–1349.

Thinakaran, G., Borchelt, D.R., Lee, M.K., Slunt, H.H., Spitzer, L., Kim, G., Rotovitsky, T., Davenport, F., Nordstedt, C., Seeger, M., et al. (1996). Endoproteolysis of presenilin 1 and accumulation of processed derivatives in vivo. Neuron *17*, 181–190.

Thinakaran, G., Harris, C.L., Ratovitski, T., Davenport, F., Slunt, H.H., Price, D.L., Borchelt, D.R., and Sisodia, S.S. (1997). Evidence that levels of presenilins (PS1 and PS2) are coordinately regulated by competition for limiting cellular factors. J. Biol. Chem. *272*, 28415–28422.

Tomita, T., Maruyama, K., Saido, T.C., Kume, H., Shinozaki, K., Tokuhiro, S., Capell, A., Walter, J., Grunberg, J., Haass, C., et al. (1997). The presenilin 2 mutation (N141I) linked to familial Alzheimer disease (Volga German families) increases the secretion of amyloid β protein ending at the 42nd (or 43rd) residue. Proc. Natl. Acad. Sci. USA *94*, 2025–2030.

Tomita, T., Tokuhiro, S., Hashimoto, T., Aiba, K., Saido, T.C., Maruyama, K., and Iwatsubo, T. (1998). Molecular dissection of domains in mutant presenilin 2 that mediate overproduction of amyloidogenic forms of amyloid beta peptides. Inability of truncated forms of PS2 with familial Alzheimer's disease mutation to increase secretion of Abeta42. J. Biol. Chem. *273*, 21153–21160.

Tomita, T., Tokikawa, R., Morchashi, Y., Takasugi, N., Saido, T.C., Maruyama, K., and Iwatsubo, T. (1999). Carboxyl terminus of presenilin is required for overproduction of amyloidogenic Aβ42 through stabilization and endoproteolysis of presenilin. J. Neurosci. *19*, 10627–10634.

Verhage, M., Maia, A., Plomp, J., Brussaard, A., Heeroma, J., Vermeer, H., Toonen, R., Hammer, R., van den Berg, T., Missler, M., et al. (2000). Synaptic assembly of the brain in the absence of neurotransmitter secretion. Science *287*, 864–869.

Wittenburg, N., Eimer, S., Lakowski, B., Rohrig, S., Rudolph, C., and Baumeister, R. (2000). Presenilin is required for proper morphology and function of neurons in *C. elegans*. Nature *406*, 306–309.

Wolfe, M.S., Xia, W., Ostaszewski, B.L., Diehl, T.S., Kimberly, W.T., and Selkoe, D.J. (1999). Two transmembrane aspartates in presenilin-1 required for presenilin endoproteolysis and γ-secretase activity. Nature *398*, 513–517.

Xu, X., Shi, Y., Wu, X., Gambett, P., Sui, D., and Cui, M. (1999). Identification of a novel PSD-95/Dlg/Zo-1 (PDZ)-like protein interacting with the C-terminus of presenilin-1. J. Biol. Chem. *274*, 32543–32546.

Yu, H., Kessler, J., and Shen, J. (2000). Heterogeneous populations of ES cells in the generation of a floxed *Presenilin-1* allele. Genesis *26*, 5–8.

Zaman, S., Parent, A., Laskey, A., Lee, M., Borchelt, D., Sisodia, S., and Malinow, R. (2000). Enhanced synaptic potentiation in transgenic mice expressing presenilin-1 familial Alzheimer's disease mutation is normalized with a benzodiazepine. Neurobiol. Dis. *7*, 54–63.

Zhang, Z., Lee, C., Mandiyan, V., Borg, J., Margolis, B., Schlessinger, J., and Kuriyan, J. (1997). Sequence-specific recognition of the internalization motif of the Alzheimer's amyloid precursor protein by the X11 PTB domain. EMBO J. *16*, 6141–6150.

Zhang, Z., Nadeau, P., Song, W., Donoviel, D., Yuan, M., Bernstein, A., and Yankner, B. (2000). Presenilins are required for γ-secretase cleavage of β-APP and transmembrane cleavage of Notch-1. Nat. Cell Biol. *2*, 463–465.